

## The Analysis of the Influence of the Ferromagnetic Rod in an Annular Magnetohydrodynamic (MHD) Pump

Nassima Bergoug<sup>1</sup>, Fatima Zohra Kadid<sup>1</sup>, Rachid Abdessemed<sup>1</sup>

**Abstract:** This paper deals with the 2D modelisation of an annular induction magnetohydrodynamic (MHD) pump using finite volume method in cylindrical coordinates and taking into consideration the saturation of the ferromagnetic material. The influence of the ferromagnetic rod on the different characteristics, in the channel of the MHD pump was studied in the paper.

**Keywords:** Annular channel, Induction pump, Magnetohydrodynamic (MHD), Navier Stokes equations, Finite volume method, Ferromagnetic rod.

### 1 Nomenclature

$A$  – Magnetic vector potential [Tm];

$B$  – Magnetic induction [T];

$D$  – Electric flux density [C/m<sup>2</sup>];

$J$  – Electric conduction current density [A/m<sup>2</sup>],  $J_{ex} = J + J_{in}$  ;

$J_{in}$  – Induced current density [A/m<sup>2</sup>];

$J_{ex}$  – Electrical current density source density [A/m<sup>2</sup>];

$V$  – Flow velocity [m/s];

$F$  – Electromagnetic force density [N/m<sup>3</sup>];

$\sigma$  – Electric conductivity [ $\Omega^{-1}m^{-1}$ ];

$\mu$  – Magnetic permeability [H/m];

$\nu$  – Kinematic viscosity coefficient [m<sup>2</sup>/s];

$p$  – The pressure of the fluid;

$\xi(r, z)$  – Vorticity vector;

$\Psi(r, z)$  – Vector potential hydrodynamic.

---

<sup>1</sup>L.E.B. Research Laboratory, Electrical engineering department; University of Batna, 05000 Batna, Algeria;  
E-mails: nassimal\_elt@yahoo.fr; Fzohra\_kadid@hotmail.com; rachid.abdessemed@gmail.com

## **1 Introduction**

Magnetohydrodynamic (MHD) is the theory of the interaction of electrically conducting fluids and electromagnetic fields. Application arises in astronomy and geophysics as well as in connection with numerous engineering problems, such as liquid metal cooling of nuclear reactors, electromagnetic casting of metals, MHD power generation and propulsion [1].

The pumping of liquid metal may use an electromagnetic device, which induces eddy currents in the metal. These induced currents and their associated magnetic field generate the Lorentz force whose effect can be actually the pumping of the liquid metal [2, 3].

Magnetohydrodynamics is widely applied in various domains, such as metallurgical industry, the transport or the pumping of the liquid metals in fusion and the marine propulsion [4, 5]. The advantage of these pumps which ensure the energy transformation is the absence of moving parts. The interaction of moving conducting fluids with electric and magnetic fields allows for a rich variety of phenomena associated with electro-fluid-mechanical energy conversion [6].

In the previous work [7] we studied the 2D electromagnetic phenomena in a MHD pump by the finite volume method in harmonic mode. The different characteristics of the MHD pump (vector potential, magnetic induction, currents density and the electromagnetic force) were obtained in [7].

In this work we studied the influence of the ferromagnetic rod in the MHD pump using the finite volume method, the vector vorticity  $\xi$  and the stream function  $\psi$ . This formulation facilitates resolving the Navier Stokes's equations easily.

## **2 Description of the Induction MHD Pump**

The electromagnetic pump for a liquid metal was considered in the paper. A schematic view of the pump is shown in Fig. 1. The liquid metal flows along a channel with a cylindrical geometry of annular cross section. A ferromagnetic core is placed on the inner and the outer sides of the channel [2].

The principle of the MHD pump (Fig. 1) is similar to that of the asynchronous motor, i.e. the alimentation of the inductor creates a magnetic field  $\mathbf{B}$  sliding with the velocity of synchronism, where electric currents are induced in the liquid metal by means of a magnetic field, producing an electromagnetic force density  $\mathbf{J} \times \mathbf{B}$  with the instantaneous field ensuring the flows of the fluid [8].

The currents of the windings generate the sliding magnetic field which produces a current in the liquid metal. As a consequence a Lorentz force acting on the fluid is obtained.

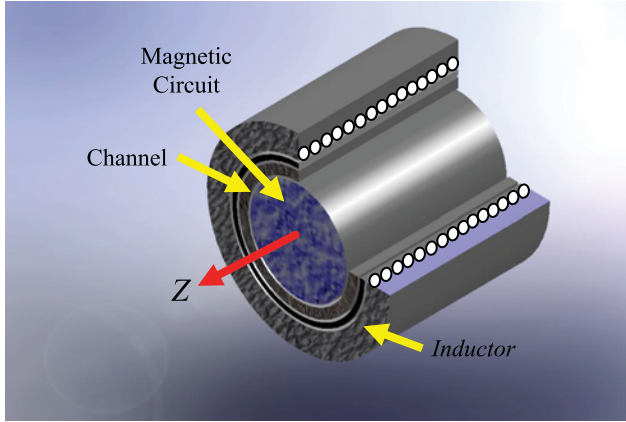


**Fig. 1** – Schematic view of the MHD pump.

The MHD pump dimensions and the properties of the mercury are given respectively in **Tables 1** and **2**.

**Table 1**  
*Dimensions of the MHD pump.*

Parameter	Values
Channel's length	40cm
Channel's width	2cm
Inductor width	20cm
Inductor length	40cm
Width of the air-gap	4mm

**Table 2**  
*Fluid properties.*

Parameter	Mercury solution
Density $\rho$	$13.6 \cdot 10^3 \text{ kg/m}^3$
Electric conductivity $\sigma$	$1.06 \cdot 10^6 \text{ } \Omega^{-1}\text{m}^{-1}$
Viscosity $\nu$	$0.11 \cdot 10^{-6} \text{ m}^2/\text{s}$
Electrical current density $J_{\text{ex}}$	$4 \cdot 10^6 \text{ A/m}^2$

### 3 Mathematical Analysis of Electromagnetics and Hydrodynamics

The Maxwell's equations applied to a pump give the following equation:

$$\text{rot} \left( \frac{1}{\mu} \text{rot} \mathbf{A} \right) = \mathbf{J}_{\text{ex}} - \sigma \left( \frac{\partial \mathbf{A}}{\partial t} - \mathbf{V} \times \text{rot} \mathbf{A} \right), \quad (1)$$

where  $\mathbf{A} = A_0 \hat{\theta}$  is the magnetic vector potential and  $\mathbf{J}_{\text{ex}} = J_{\text{ex}} \hat{\theta}$  electrical current density.  $\mathbf{V}$  is the velocity of the fluid.

The induction magnetic and the electromagnetic force density are given by:

$$\mathbf{B} = \text{rot} \mathbf{A}, \quad (2)$$

$$\mathbf{F} = \mathbf{J} \times \mathbf{B}. \quad (3)$$

Following developments in cylindrical coordinates: if two-dimensional (2D) where the current density and the magnetic vector potential are perpendicular to the longitudinal section of the MHD pump, the equation becomes:

$$\frac{\partial}{\partial z} \left( \frac{1}{r\mu} \frac{\partial A}{\partial z} \right) + \frac{\partial}{\partial r} \left( \frac{1}{r\mu} \frac{\partial A}{\partial r} \right) = -J_{\text{ex}} + \frac{\sigma}{r} \left( \frac{\partial A}{\partial t} + V_z \frac{\partial A}{\partial z} \right), \quad A = rA_0. \quad (4)$$

The equations describing the pumping process in the channel are the momentum conservation equation for laminar incompressible flows are as follows:

$$\frac{\partial \mathbf{V}}{\partial t} + (\mathbf{V} \cdot \nabla) \mathbf{V} = -\frac{1}{\rho} \text{grad} p + \nu \Delta \mathbf{V} + \frac{\mathbf{F}}{\rho}, \quad (5)$$

$$\text{div} \mathbf{V} = 0, \quad (6)$$

where  $\mathbf{V}$  stands for vector velocity,  $p$  the pressure of the fluid,  $\nu$  the kinematic viscosity of the fluid,  $\mathbf{F}$  the Lorentz force density which is given by (3) and  $\rho$  the fluid density.

The difficulty is that in the previous equations pressure and velocity are the unknown parameters. The elimination of pressure from the equations leads to a vorticity-stream function which is one of the most popular methods for solving the 2-D incompressible Navier-Stokes equations [8, 12]:

$$\xi = \text{rot} \mathbf{V}, \quad \mathbf{V} = \text{rot} \boldsymbol{\psi}, \quad \boldsymbol{\psi} = \psi_0 \hat{\theta}, \quad \xi = \xi_0 \hat{\theta}, \quad (7)$$

$$\xi_{\theta} = \frac{\partial V_r}{\partial z} - \frac{\partial V_z}{\partial r}, \quad (8)$$

$$V_r = -\frac{1}{r} \frac{\partial \psi}{\partial z}, \quad V_z = \frac{1}{r} \frac{\partial \psi}{\partial r}, \quad \psi = r \psi_{\theta}. \quad (9)$$

Using these new dependent variables, the two momentum equations can be combined (thereby eliminating pressure) to give:

$$\begin{aligned} \nu \left[ \frac{\partial^2 \xi_{\theta}}{\partial r^2} + \frac{\partial^2 \xi_{\theta}}{\partial z^2} + \frac{1}{r} \frac{\partial \xi_{\theta}}{\partial r} - \frac{\xi_{\theta}}{r^2} \right] = \\ = \frac{\partial \xi_{\theta}}{\partial t} + \frac{\partial \xi_{\theta}}{\partial r} V_r + \frac{\partial \xi_{\theta}}{\partial z} V_z + \frac{V_r}{r} \xi_{\theta} + \frac{1}{\rho} \left( \frac{\partial F_z}{\partial r} - \frac{\partial F_r}{\partial z} \right). \end{aligned} \quad (10)$$

An additional equation involving the new dependant variables  $\xi$  and  $\psi$  can be obtained by substituting (8) into (9) which give:

$$\frac{1}{r} \left[ \frac{\partial^2 \psi}{\partial z^2} + \frac{\partial^2 \psi}{\partial r^2} \right] = -\xi_{\theta}. \quad (11)$$

In order to determine the pressure, it is necessary to solve an additional equation which is referred to as the Poisson equation for pressure; the latter is obtained by differentiating (5):

$$\Delta p = \frac{2\rho}{r^2} \left[ \frac{\partial^2 \psi}{\partial z^2} \frac{\partial^2 \psi}{\partial r^2} \right]. \quad (12)$$

#### 4 Numerical Method and Results

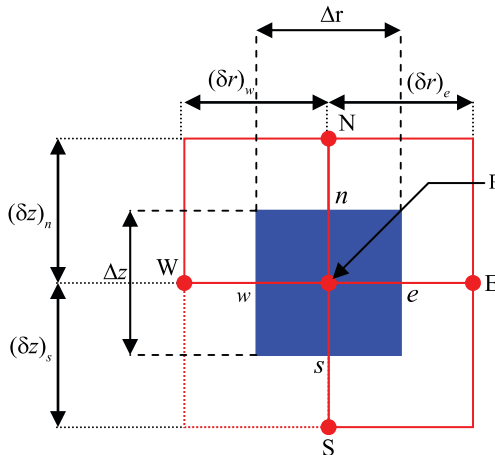


Fig. 2 – Discretisation in finite volume method.

The method consists of discretising differential equations by integration on finite volumes surrounding the nodes of the grid.

In this method, each principal node P is surrounded by four nodes N, S, E and W located respectively at North, South, East and West (Fig. 2) [11].

We integrate the electromagnetic and Navier Stokes equation in the finite volume delimited by the surfaces E, W, N and S:

$$\begin{aligned} & \iint_{z,r} \left[ \frac{\partial \xi_{\theta 0}}{\partial t} + \frac{\partial \xi_{\theta 0}}{\partial r} V_r + \frac{\partial \xi_{\theta 0}}{\partial z} V_z + \frac{V_r}{r} \xi_{\theta 0} \right] dr dz = \\ & = \iint_{z,r} \nu \left[ \left[ \frac{\partial^2 \xi_{\theta 0}}{\partial r^2} + \frac{\partial^2 \xi_{\theta 0}}{\partial z^2} + \frac{1}{r} \frac{\partial \xi_{\theta 0}}{\partial r} - \frac{\xi_{\theta 0}}{r^2} \right] + \frac{1}{\rho} \left( \frac{\partial F_z}{\partial r} - \frac{\partial F_r}{\partial z} \right) \right] dr dz. \end{aligned} \quad (13)$$

Finally we obtained the algebraic equation which is written as:

$$a_p \xi_p = a_E \xi_E + a_w \xi_w + a_N \xi_N + a_S \xi_S + d_p, \quad (14)$$

$$\begin{aligned} a_p &= a_E + a_w + a_N + a_S + d_p, \\ a_E &= \left( -\frac{1}{2} (V_r)_E + \frac{\nu_E}{(\partial r)_E} + \frac{1}{2} \frac{\nu_E}{r_E} \right) \Delta t \Delta z, \\ a_w &= \left( -\frac{1}{2} (V_r)_W + \frac{\nu_W}{(\partial r)_W} - \frac{1}{2} \frac{\nu_W}{r_W} \right) \Delta t \Delta z, \\ a_N &= \left( -\frac{1}{2} (V_z)_N + \frac{\nu_N}{(\partial z)_N} \right) \Delta t \Delta r, \\ a_S &= \left( -\frac{1}{2} (V_z)_S + \frac{\nu_S}{(\partial z)_S} \right) \Delta t \Delta r, \\ d_p &= a_p^0 \Delta r \Delta z. \end{aligned} \quad (15)$$

After the resolution of the equation (14) we obtain the matrix in the form:

$$[M][\xi] = [D], \quad (16)$$

where:

$[M]$ : Matrix Coefficients,

$[\xi]$ : Vector vorticity Matrix,

$[D]$ : Vector source Matrix.

The same resolution is done for the electromagnetic equation (4). After integration using the finite volume method we obtain the system as:

$$[M + jL][A] = [J_{ex}], \quad (17)$$

where:

$[M + jL]$ : Matrix Coefficients,

$[A]$ : Vector Potential Matrix,

$[J_{ex}]$ : Vector source Matrix.

The Fig. 3 represents the annular MHD pump in the plan  $(r, z)$  with the boundary conditions.

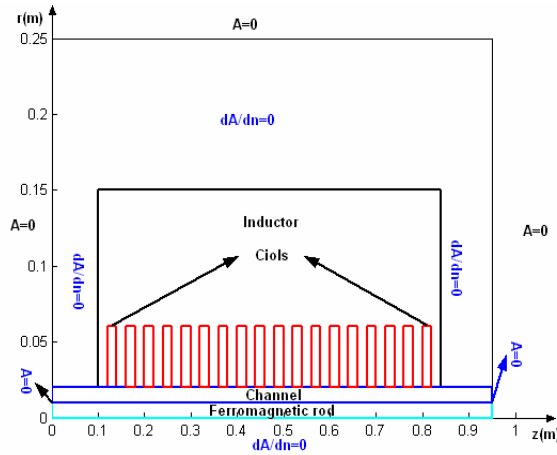


Fig. 3 – Numerical model of the annular MHD pump.

With the Dirichlet boundary and the Neumann conditions  $A = 0$ ,  $\frac{\partial A}{\partial n} = 0$  the resolution is done according to an iterative process.

The Figs. 5, 6, 7 and 8, represent the equipotential lines with and without ferromagnetic rod, the distribution of the vector potential  $A$  and the magnetic induction  $B$  in the MHD pump.

The Figs. 9 and 10 below represent the variation of the electromagnetic force and the velocity in the channel with and without ferromagnetic rod in the MHD pump.

Velocity of the fluid passes through a transitional period and then stabilizes as all the electrical machines. It is within that velocity increases as we advance in the channel.

The obtained results are in agreement qualitatively with those obtained by [5]. Comparison of the results of velocity with and without ferromagnetic rod suggests that velocity of the fluid increases, which is due to the presence of the

ferromagnetic rod with allows maximum of the electromagnetic force to propel the fluid in the channel.

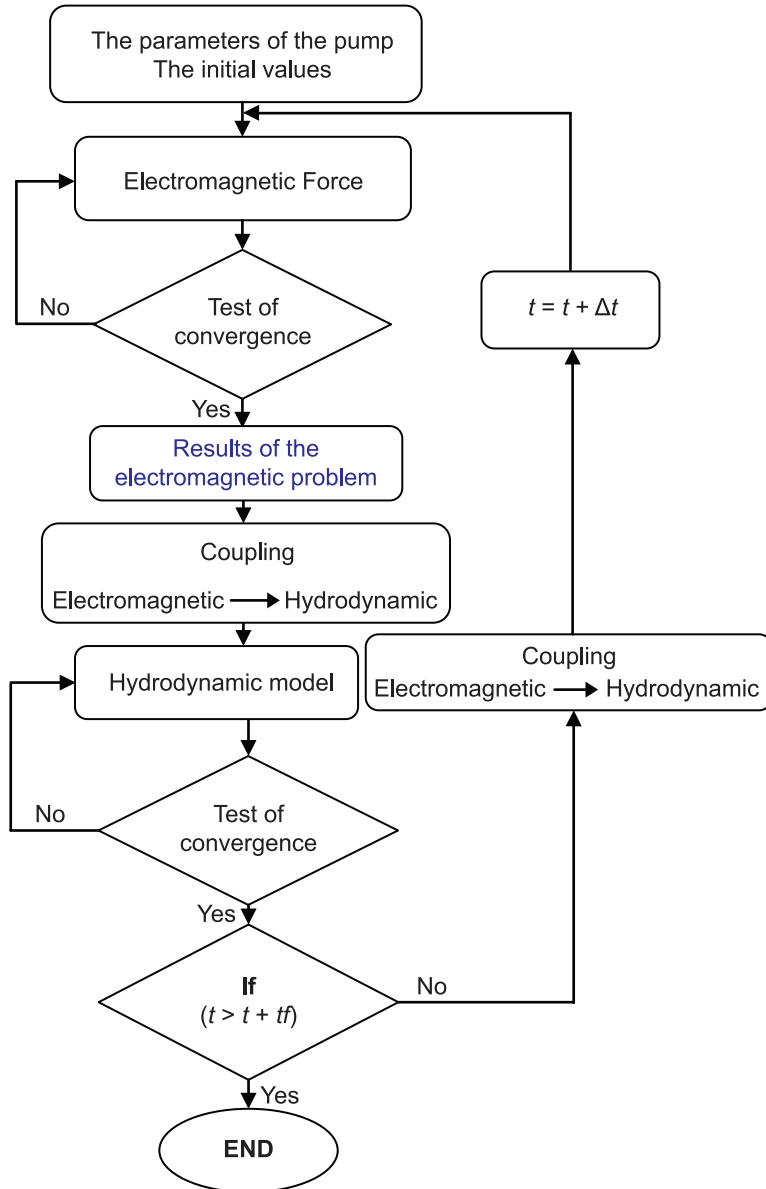
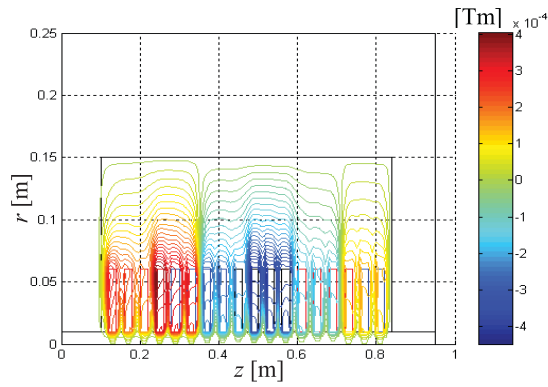
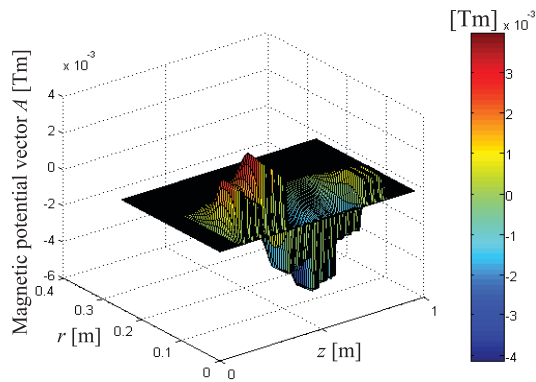


Fig. 4 – Computation algorithm





**Fig. 5** – Distribution of the magnetic vector potential without ferromagnetic rod in the MHD pump.



**Fig. 6** – Distribution of the magnetic vector potential  $A$ .

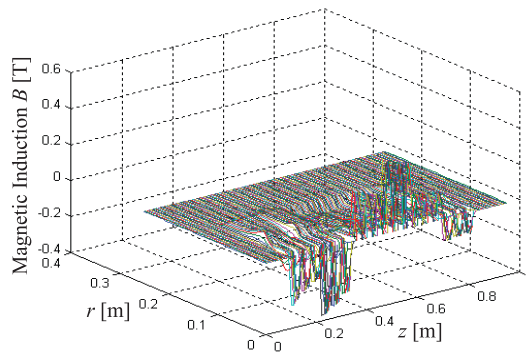


**Fig. 7** – Magnetic induction in the MHD pump.

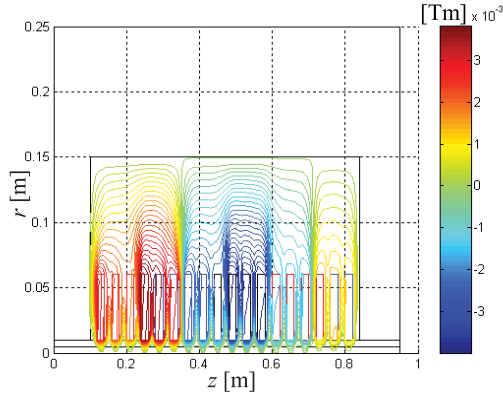


**Fig. 8** – Distribution of the magnetic vector potential *A* with ferromagnetic rod in the MHD pump.

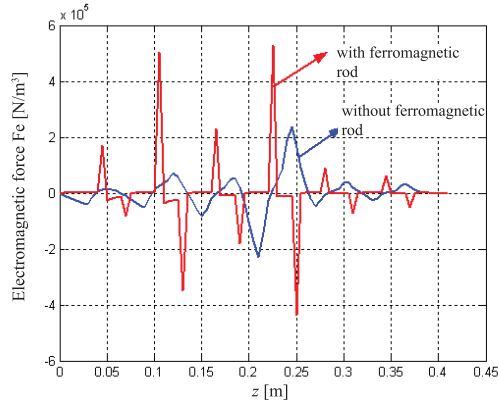


**Fig. 9** – Force electromagnetic distribution without and with ferromagnetic rod in the channel of the MHD pump.

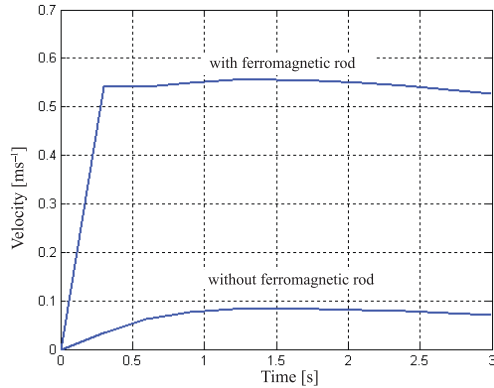


**Fig. 10** – Velocity distribution without and with ferromagnetic rod in the channel of the MHD pump.

## 5 Conclusion

The influence of the ferromagnetic rod on different characteristics of the induction MHD pump was studied.

The introduction of the plate allows for reinforcing the magnetic field, whereby the current density, electromagnetic force and velocity become important in the channel.

The obtained results confirm the influence of the ferromagnetic rod on the velocity distribution in the investigated flow and are in full agreement with those carried out by [5] and [6], provided that the results are obtained in different working conditions.

## 7 References

- [1] L. Leboucher, P. Marty, A. Alemany, P. Masse: An Inverse Method in Electromagnetism Applied to the Optimization of Inductors, IEEE Transactions on Magnetics, Vol. 28. No. 5, Sept. 1992, pp. 3330 – 3332.
- [2] R. Berton: Magnétohydrodynamique, Masson, Paris, France, 1991.
- [3] C.A. Borghi, A. Cristofolini, M. Fabbri: Study of the Design Model of a Liquid Metal Induction Pump, IEEE Transactions on Magnetics, Vol. 34. No. 5, Sept. 1998, pp. 2956 – 2959.
- [4] N. Takorabet: Computation of Force Density Inside the Channel of an Electromagnetic Pump by Hermite Projection, IEEE Transactions on Magnetics, Vol. 42, No. 3, March 2006, pp.430 – 433.
- [5] M. Ghassemi, H. Rezaeinezhad, A. Shahidian: Analytical Analysis of Flow in a Magneto-hydrodynamic Pump (MHD), 14th Symposium on Electromagnetic Launch Technology, Victoria, Canada, 10 – 13 June 2008.
- [6] A. Affanni, G. Chiorboli: Numerical Modelling and Experimental Study of an AC Magneto-hydrodynamic (MHD) Micropump, Instrumentation and Measurement Technology Conference, Sorrento, Italy, 24 – 27 April 2006, pp.2249 – 2253.
- [7] N. Bergoug, F.Z. Kadid, R. Abdessemed: The Influence of the Ferromagnetic Materials on the Performances of an Annular Induction Magneto-hydrodynamic (MHD) Pump, International Conference on Electrical Engineering Design and Technologies, Hammamet, Tunisia, 04 – 06 Nov. 2007.
- [8] F.Z. Kadid, R. Abdessemed, S. Drid: Study of the Fluid Flow in a MHD Pump by Coupling Finite Element-Finite Volume Computation, Journal of Electrical Engineering, Vol. 55, No.11-12, Nov/Dec. 2004, pp. 301 – 305.
- [9] G.S. Park, K. Seo: A Study on the Pumping Force of the Magnetic Fluid Linear Pump, IEEE Transactions on Magnetics, Vol. 39, No.3, May 2003, pp. 1468 – 1471.
- [10] N. Shamsuddeen, A. Ashok, J. Rajendrakumar, V. Krishna, V. Jayashankar: Design and Analysis of Annular Linear Induction Pump, Joint International Conference on Power System Technology and IEEE Power India Conference, New Delhi, India, 12 – 15 Oct. 2008.
- [11] S.V. Patankar: Numerical Heat Transfer Fluid Flow, Taylor and Francis, New York, USA, 1980.
- [12] S.K. Krzeminski, A. Cala M. Smialek: Numerical Simulation of 2D MHD Flows  $\psi$ - $\xi$ -A Method, IEEE Transactions on Magnetics, Vol. 32, No. 3, May 1996, pp. 990 – 993.